Adsorption distance of S on Ni(001): An electron-energy-loss-spectroscopy cross-section analysis of the Ni(001)-$c(2\times2)$S system

Z. Q. Wu, Y. Chen, M. L. Xu,* and S. Y. Tong
Department of Physics and Laboratory for Surface Studies, University of Wisconsin–Milwaukee, P.O. Box 413, Milwaukee, Wisconsin 53201

S. Lehwald, M. Rocca,† and H. Ibach
Institut für Grenzflächenforschung und Vakuumphysik, Kernforschungsanlage Jülich, Postfach 1913, D-5170 Jülich, Federal Republic of Germany

(Received 23 May 1988)

The inelastic-electron-scattering cross sections of surface and antinode adsorbate-induced bulk phonons are calculated for the Ni(001)-$c(2\times2)$S system. The calculated cross sections are sensitive to variations in the incident electron energy, phonon $\mathbf{q}_{\parallel}$, and the spacing between S and Ni layers. By comparing calculated cross sections with measured electron-energy-loss spectra at different electron energies and phonon $\mathbf{q}_{\parallel}$ vectors, we determined the S-Ni spacing unambiguously at 1.35 Å. An *ad hoc* non-central-force model was introduced to explain the measured dispersion curves.

I. INTRODUCTION

Recently, there has been much progress in the analysis of vibrational motion of atoms on clean and adsorbate-covered surfaces by inelastic He scattering[1] and inelastic electron scattering.[2,3] In the case of inelastic electron scattering, a major advance is the ability of microscopic multiple-scattering theory[4–6] to quantitatively calculate the electron-energy-loss cross sections [or electron-energy-loss-spectroscopy (EELS) cross sections] of surface and bulk modes of a system covering a wide range of electron energies (30–350 eV). Such an analysis has recently been done for Ni(001),[7,8] Ni(110),[9] Cu(001),[10] and Cu(111).[11] In this paper we present a detailed cross-section analysis for the Ni(001)-$c(2\times2)$S system. In an earlier paper we have shown that surface modes and antinode adsorbate-induced bulk modes have large inelastic-electron-scattering cross sections.[12] The cross sections of these modes are sensitive to variations in momentum transfer $\mathbf{q}_{\parallel}$, incident electron energy, and the scattering geometry.[4–12] We show in this paper that the relative intensities of the modes are accurate indicators of the S-Ni spacing and that by comparing data with the calculated EELS cross sections, the S-Ni spacing can be quantitatively determined. This determination is unambiguous in spite of the fact that the correct lattice dynamical model for this system may not be known. The reason for this selective sensitivity of EELS cross sections to surface spacings over atomic displacement amplitudes is as follows. Modes that have large inelastic scattering cross sections generally have significant (perpendicular or parallel) atomic displacements in the first two to three surface layers.[13] The short electron mean free path also biases in favor of the top surface layers.[14] Therefore, the EELS cross section is dominated by the interference of phonon-loss vertices between the first three layers. By changing the S-Ni spacing, the phases of electron wave functions between these layers are varied by large amounts. These changes dominate over variations in the eigendisplacements due to different lattice dynamical results. We shall show this explicitly in Sec. IV.

The organization of the remainder of this paper is as follows. In Sec. II, we present the experimental measurements. The dynamical model for an inelastic-electron-phonon-scattering calculation is given in Sec. III. Lattice dynamical models and dispersion relations for the Ni(001)-$c(2\times2)$ system are given in Sec. IV. Comparison between theory and experiment for the EELS cross sections as a function of electron energy and phonon wave vector $\mathbf{q}_{\parallel}$ as well as the determination of the S-Ni spacing are given in Sec. V. Section VI is a summary.

II. EXPERIMENTAL MEASUREMENT

The experimental details of sample and sulfur-overlayer preparation were the same as in a recent paper of Lehwald *et al.*[15] where the dispersion curves for the Ni(001)-$c(2\times2)$S system have been measured. Briefly, the Ni single crystal was cleaned by repeated cycles of Ne-ion bombardment and annealing to 1400 K until the crystal was leached of carbon and sulfur and no traces of either impurity could be detected neither by Auger nor by EELS. The $c(2\times2)$ sulfur layer was obtained by exposing the sample to H_2S with the sample temperature held at 500 K. The sulfur surface coverage saturated after an exposure of ~ 15 Langmuire and saturation corresponding to a peak-to-peak ratio in the Auger spectrum of $I_{S_{152}}/I_{Ni_{848}}=1.0$. A sharp $c(2\times2)$ low-energy electron diffraction (LEED) pattern was observed after this treatment.

In contrast to Ref. 15, the electron-energy-loss spectra were now recorded using an improved version of the double-pass electron spectrometer, the energy dispersive elements and the lens system of which had been opti-

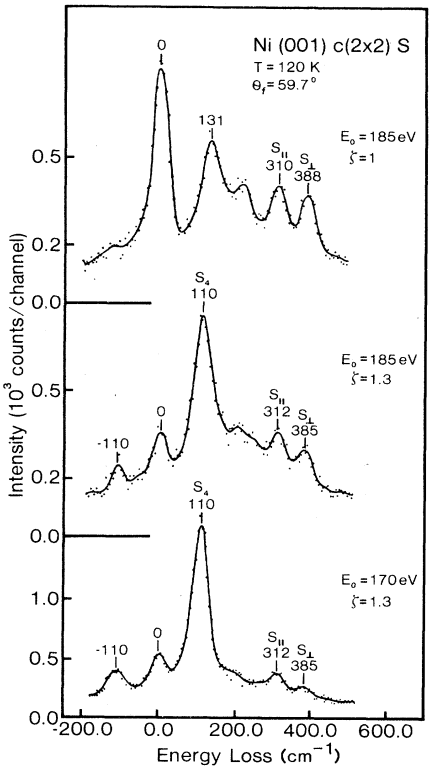

FIG. 1. Typical off-specular electron-energy-loss spectra on Ni(001)-$c(2\times2)$S recorded with an impact energy of 185 eV at $\zeta=1$ ($\bar{X}$ point) and $\zeta=1.3$ and for 170 eV at $\zeta=1.3$. The energy resolution is 42 cm^{-1}.

mized with the help of trajectory calculations.[16] The spectrometer also featured an improved calibration of the scattering angles. The scattering plane was aligned along with the surface normal and the [110] direction ($\bar{\Gamma}\bar{X}$). Compared to the earlier paper[15] where the loss spectra were recorded with an energy resolution of 60 cm^{-1} in the elastic peak and with typical count rates of $\lesssim 20$ counts/sec in the loss peak, the spectrometer now was allowed to have typically 100 counts/sec in the loss peaks with the energy resolution set to 40–45 cm^{-1}.

Spectra were recorded for impact energies E from 150 to 190 eV in steps of 5 eV for two points within the surface Brillouin zone each: at $\zeta=1$ ($\bar{X}$ point, $\zeta=q_{\parallel}/1.26$ $Å^{-1}$) and at $\zeta=1.3$. The exit angle θ_f was adjusted to 59.7° off the surface normal. The data were sampled at 5-cm^{-1} intervals with a total sampling time of 15 sec/channel. The temperature of the sample was held at 120 K. Three typical loss spectra are shown in Fig. 1. Further details are presented and discussed in Sec. V.

III. INPUTS FOR MULTIPLE-SCATTERING CALCULATION OF EELS CROSS SECTIONS

The microscopic method we used to calculate EELS cross sections is based on the rigid-ion multiple-scattering slab model.[4–7] Since the experimental measurements were taken at rather high energies, 150–190 eV, the electrons scatter off mainly the near-core region of atoms. Hence, we expect the cross-section calculations to be rather accurate. Earlier applications of this method to different faces of Ni and Cu have produced remarkably good fits to the data.[7–11] For dynamical inputs of the Ni(001)-$c(2\times2)$S system, we used the same Ni phase shifts, inner potential ($V_0=10.5$ eV), inelastic damping

$$V_I=3.8\times\left[\frac{E+V_0}{90+V_0}\right]^{1/3}\text{ eV}$$

as those used earlier for clean Ni(001).[13,17,18] The S-phase shifts used were the same as those in earlier LEED (Refs. 17–19) and photoelectron diffraction calculations.[20] In other words, the dynamical inputs were fixed by their values in previous calculations. The remaining inputs were the layer-by-layer displacement amplitudes of the S and Ni atoms. These we obtain from lattice dynamical calculations described in Sec. IV.

IV. DISPLACEMENT AMPLITUDES AND PHONON DISPERSION

The phonon-dispersion curves for the Ni(001)-$c(2\times2)$S system have been recently measured by Lehwald *et al.*[15] A loss peak at 350 cm^{-1} at $\bar{\Gamma}$ was attributed to the frequency of the $S_{\perp}$ mode. The measured dispersion behavior was well reproduced in a nearest-neighbor central-force lattice dynamical model with the S atoms placed at fourfold hollow sites and the S-Ni spacing put at 1.45 Å.[15] If the S-Ni spacing is changed to 1.35 Å, the nearest-neighbor central-force calculation shows a gap of 17 cm^{-1} near $\bar{\Gamma}$ between the $S_{\perp}$ and $S_{\parallel}$ (even) modes (see Fig. 3). Also, these modes cross over in frequency in the Brillouin zone between $\bar{\Gamma}$ and $\bar{X}$. Based on these results, Lehwald *et al.*[15] suggested that the measured dispersion curves could only be reconciled with an adsorption model in which the S atoms are 1.45 Å (perpendicular distance) from the Ni atoms below.

However, it is well known that lattice dynamical results based on parametrized force-constant models are not unique. For example, by introducing noncentral forces between S and Ni atoms, we can keep the S-Ni spacing at 1.35 Å and still obtain calculated dispersion curves that are practically indistinguishable from those of nearest-neighbor central forces with $d_{\text{S-Ni}}=1.45$ Å.[21] Only within the nearest-neighbor central force model do the dispersion curves couple directly to the S-Ni spacing. If noncentral forces or forces between more distant neighbors are introduced, the additional parameters decouple the dispersion relations from bond distances of surface atoms. Dispersion curves from such multiparameter lattice dynamical models can no longer be used to quantitatively determine surface spacings.[22]

In Fig. 2 we show dispersion curves from $\bar{\Gamma}$ to $\bar{X}$ for a 29-layer slab based on the nearest-neighbor central force model with $d_{\text{S-Ni}}=1.45$ Å. For force constants, we used $k_{\text{Bulk}}(\text{Ni})=3.79\times10^4$ dyn/cm, $k_{12}(\text{Ni})=1.2k_B(\text{Ni})$, and $k_{\text{S-Ni}}=9.97\times10^4$ dyn/cm. These were the same values used by Lehwald *et al.*[15] The 11 surface modes (S_{1L}, S_4 even, S_4 odd, S_5 pair, S_{6L}, S_{1H}, S_{6H}, $S_{\parallel}$ even, $S_{\parallel}$ odd, and $S_{\perp}$) and the antinode adsorbate-induced bulk (AIB)

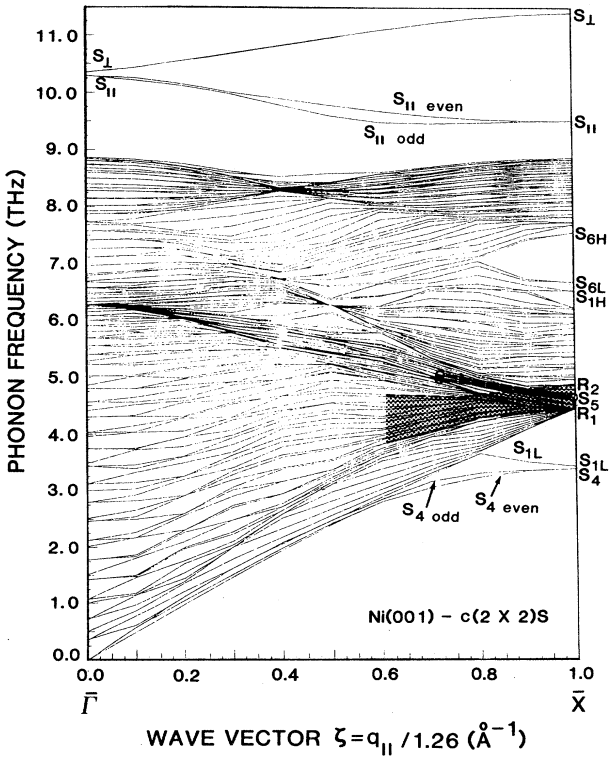

FIG. 2. Calculated phonon dispersion curves between $\bar{\Gamma}$ and $\bar{X}$ for Ni(001)-$c(2\times2)$S using a nearest-neighbor central force lattice dynamical model with $d_{\text{S-Ni}}=1.45$ Å. The shaded area represents the band of antinode adsorbate-induced bulk modes. 1 THz=33.336 cm^{-1}.

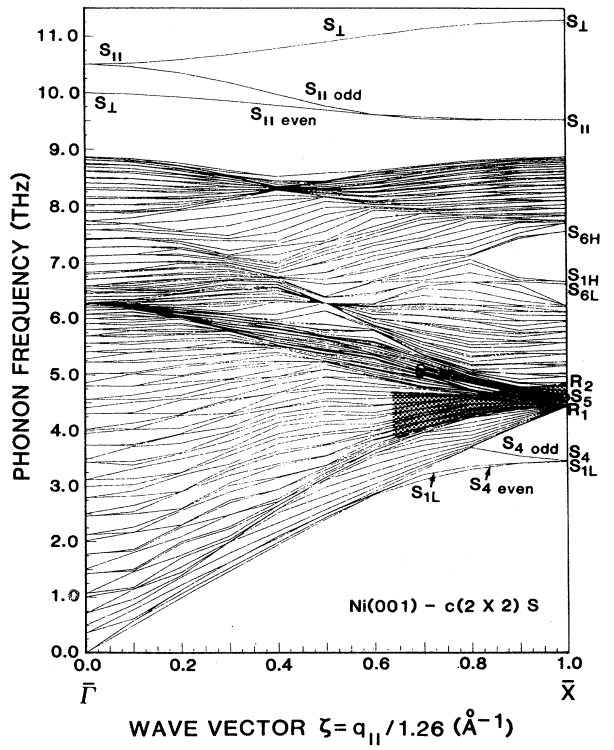

FIG. 3. Similar to Fig. 2 for $d_{\text{S-Ni}}=1.35$ Å.

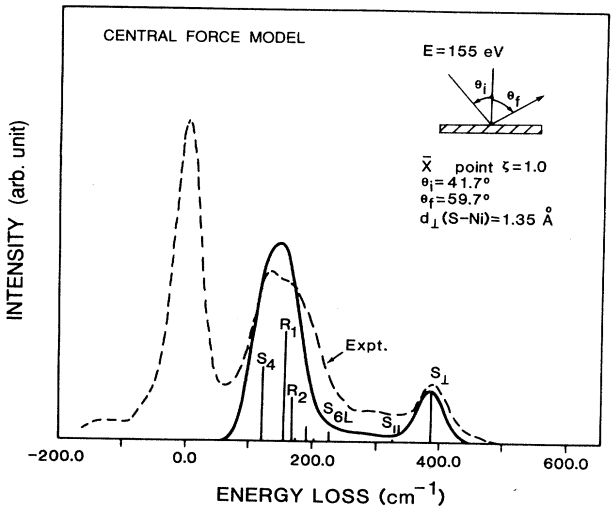

FIG. 4. Calculated (solid line) and measured (dashed line) electron-energy-loss cross-section spectra for incident electron energy $E=155$ eV and $\zeta=1.0$ ($\bar{X}$ point). Each vertical line represents individual mode scattering intensity. Only the loss side of the data is compared to the calculation. The atomic displacement amplitudes based on a central-force lattice dynamical model and $d_{\text{S-Ni}}=1.35$ Å are used for the EELS cross-section calculations.

modes R_1, R_2, are identified in the figure. The polarization and other properties of thees modes are discussed elsewhere.[12] For the scattering plane along $\bar{\Gamma}\bar{X}$, the phonon modes with large inelastic-electron-scattering cross sections are S_4 even, S_{6L}, $S_{\parallel}$ even, $S_{\perp}$, S_5 even, R_1, and R_2. The gap mode S_{6H} generally has a smaller cross section. Keeping these same force constants, we changed $d_{\text{S-Ni}}$ to 1.35 Å and obtained the dispersions in Fig. 3. Here, we noticed a reversal in the order of $\omega_{S_{\perp}}$ and $\omega_{S_{\parallel}}$ between the $\bar{\Gamma}$ and $\bar{X}$ points, but the dispersion curves depend on the lattice dynamical model. If we introduce

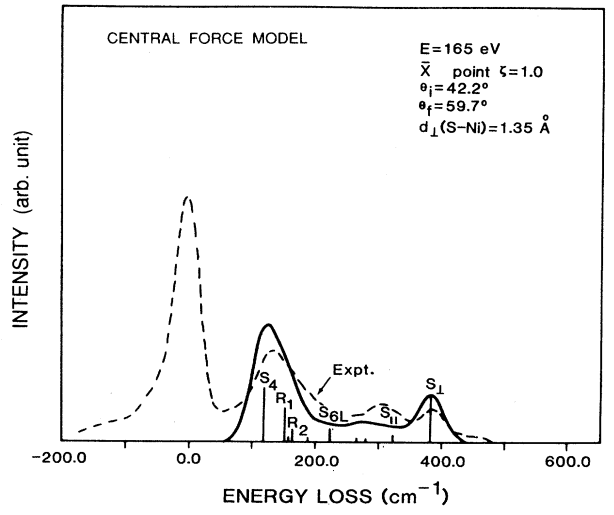

FIG. 5. Similar to Fig. 4 for $E=165$ eV.

noncentral forces between the S atom and its Ni neighbors, then we write for the diagonal matrix element of the force constant matrix

$$\phi_{ZZ} = -\alpha_{\text{N.C.}} k_{\text{S-Ni}} \cos\theta \ , \tag{1}$$

where θ is the polar angle measured from the surface of the nearest-neighbor S-Ni bond. The factor $\alpha_{\text{N.C.}}$ is the non-central-force parameter ($\alpha=1$ for the central force model). One can now adjust $\alpha_{\text{N.C.}}$ such that when the Ni-S spacing is 1.35 Å, the dispersion curves are practically those shown in Fig. 2 (for Ni-S distance $=1.45$ Å, in the central force model). The optimal value of $\alpha_{\text{N.C.}}$ is 1.15 to achieve an excellent fit to Fig. 2.

The atomic displacements at $\bar{X}$ of the surface modes S_4 even, S_{6L}, S_5 even, $S_{\parallel}$ even, and $S_{\perp}$, as well as those of the antinode AIB modes R_1, R_2 for a nine-layer slab are listed in Table I. For the electron loss spectra, we find that the Gaussian-broadened spectra of a nine-layer calculation is indistinguishable from that of a 29-layer slab. While the calculated spectra drawn in the figures correspond to results of the thicker slab, the atomic displacements listed here are for a nine-layer slab, for easier identification. The tabulated results are for: (i) central-force model, $d_{\text{S-Ni}}=1.45$ Å, (ii) central-force model, $d_{\text{S-Ni}}=1.35$ Å, (iii) non-central-force model, $d_{\text{S-Ni}}=1.35$ Å. Multiple-scattering calculations for electron-energy-loss cross sections are carried out and compared to experiment to determine the Ni-S spacing. The results are discussed in Sec. V.

V. S-Ni SPACING VIA EELS CROSS-SECTION ANALYSIS

From Sec. IV we have seen that the dispersion data of Ni(001)-$c(2\times2)$S can be fitted by results of either

TABLE I. The atomic displacement amplitudes of the surface modes S_4 even, S_{6L}, $S_{\parallel}$ even, $S_{\perp}$, S_5 even, and the antinode AIB modes R_1, R_2 at $\bar{X}$ point (e_x, [100]; e_y, [010]; e_z, towards vacuum).

Mode	Layer index	Central force model $d_{\perp}$ (S-Ni)$=1.45$ Å			Central force model $d_{\perp}$ (S-Ni)$=1.35$ Å			Non-central-force model $d_{\perp}$ (S-Ni)$=1.35$ Å		
		e_x	e_y	e_z	e_x	e_y	e_z	e_x	e_y	e_z
S_4 (even)	1	0.40	0.40	0.0	0.36	0.39	0.0	0.32	0.42	0.0
	2	0.0	0.0	0.52	0.0	0.0	0.55	0.0	0.0	0.56
	2	0.0	0.0	0.53	0.0	0.0	0.51	0.0	0.0	0.43
	3	−0.15	−0.15	0.0	−0.16	−0.15	0.0	−0.17	−0.14	0.0
	3	−0.15	−0.15	0.0	−0.15	−0.16	0.0	−0.14	−0.17	0.0
S_{6L}	1	0.0	0.0	0.46	0.0	0.0	0.45	0.0	0.0	0.50
	2	0.0	0.21	0.0	0.0	0.18	0.0	0.0	0.24	0.0
	2	0.21	0.0	0.0	0.18	0.0	0.0	0.24	0.0	0.0
	3	0.0	0.0	0.0	0.0	0.0	0.0	0.0	0.0	0.0
	3	0.0	0.0	0.64	0.0	0.0	0.67	0.0	0.0	0.60
$S_{\parallel}$ (even)	1	0.44	0.45	0.0	0.50	0.44	0.0	0.46	0.40	0.0
	2	0.0	0.0	−0.45	0.0	0.0	−0.41	0.0	0.0	−0.41
	2	0.0	0.0	−0.44	0.0	0.0	−0.46	0.0	0.0	−0.47
	3	−0.21	−0.21	0.0	−0.19	−0.22	0.0	−0.21	−0.24	0.0
	3	−0.21	−0.21	0.0	−0.22	−0.19	0.0	−0.24	−0.21	0.0
$S_{\perp}$	1	0.0	0.0	0.66	0.0	0.0	0.63	0.0	0.0	0.66
	2	0.0	−0.52	0.0	0.0	−0.54	0.0	0.0	−0.52	0.0
	2	−0.52	0.0	0.0	−0.54	0.0	0.0	−0.52	0.0	0.0
	3	0.0	0.0	0.0	0.0	0.0	0.0	0.0	0.0	0.0
	3	0.0	0.0	−0.15	0.0	0.0	−0.16	0.0	0.0	−0.15
S_5 (even)	1	0.0	0.0	0.0	0.0	0.0	0.0	0.0	0.0	0.0
	2	0.0	0.0	0.0	0.0	0.0	0.0	0.0	0.0	0.0
	2	0.0	0.0	0.0	0.0	0.0	0.0	0.0	0.0	0.0
	3	−0.63	−0.33	0.0	−0.36	−0.61	0.0	−0.68	−0.20	0.0
	3	0.33	0.63	0.0	0.61	0.36	0.0	0.20	0.68	0.0
R_1	1	0.0	0.0	0.36	0.0	0.0	0.44	0.0	0.0	0.24
	2	0.0	0.30	0.0	0.0	0.32	0.0	0.0	0.21	0.0
	2	0.30	0.0	0.0	0.32	0.0	0.0	0.21	0.0	0.0
	3	0.0	0.0	0.0	0.0	0.0	0.0	0.0	0.0	0.0
	3	0.0	0.0	−0.50	0.0	0.0	−0.51	0.0	0.0	−0.44
R_2	1	0.0	0.0	0.33	0.0	0.0	0.33	0.0	0.0	0.35
	2	0.0	0.26	0.0	0.0	0.23	0.0	0.0	0.29	0.0
	2	0.26	0.0	0.0	0.23	0.0	0.0	0.29	0.0	0.0
	3	0.0	0.0	0.0	0.0	0.0	0.0	0.0	0.0	0.0
	3	0.0	0.0	−0.30	0.0	0.0	−0.23	0.0	0.0	−0.44

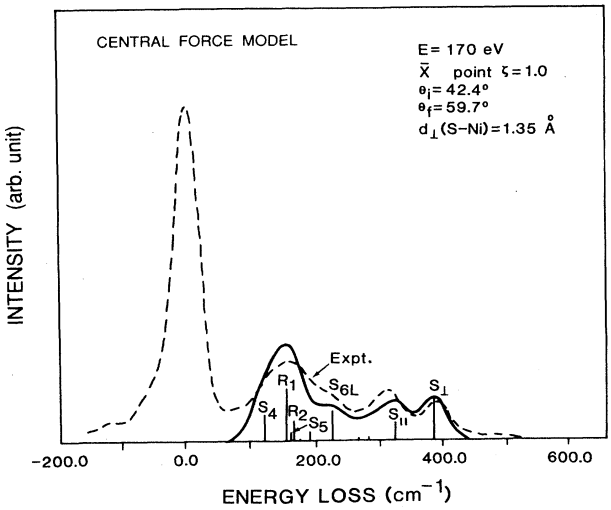

FIG. 6. Similar to Fig. 4 for $E=170$ eV.

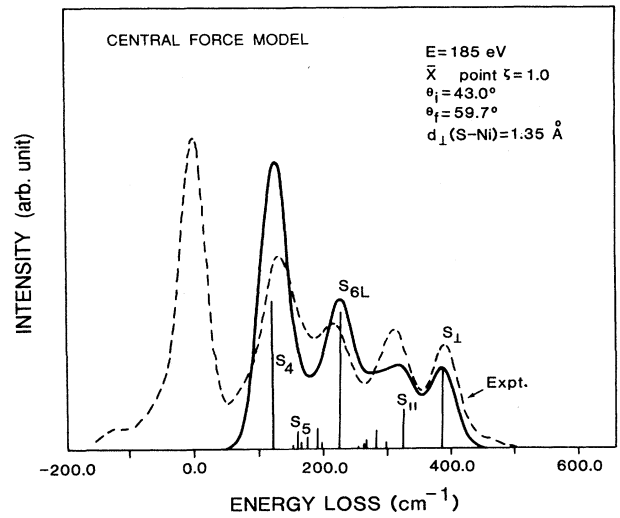

FIG. 7. Similar to Fig. 4 for $E=185$ eV.

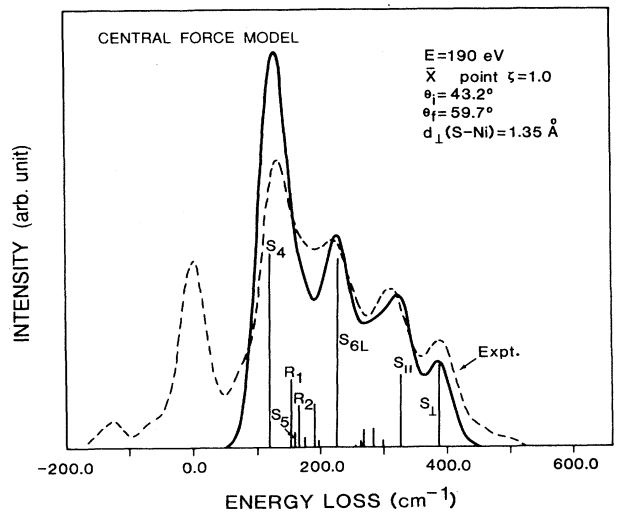

FIG. 8. Similar to Fig. 4 for $E=190$ eV.

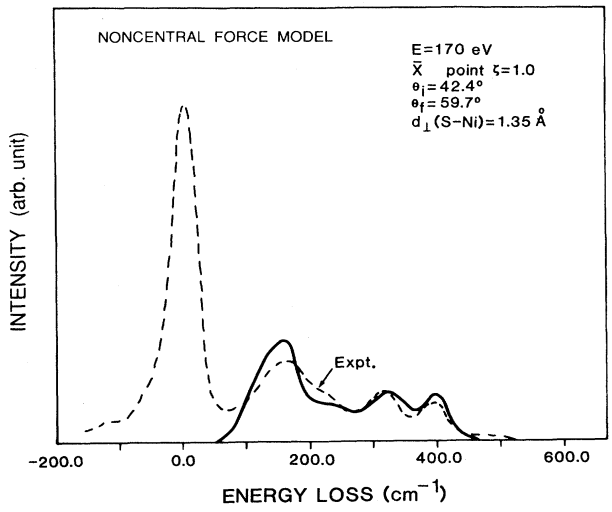

FIG. 9. Calculated (solid line) and measured (dashed line) EELS cross-section spectra for incident electron energy $E=170$ eV and $\zeta=1.0$ ($\bar{X}$ point). The atomic displacement amplitudes based on a non-central-force lattice dynamical model and $d_{\text{S-Ni}}=1.35$ Å are used for the EELS cross-section calculations.

central-force $d_{\text{Ni-S}}=1.45$ Å or non-central-force $d_{\text{Ni-S}}=1.35$ Å lattice dynamical models. Thus, it is not possible to determine the Ni-S spacing unambiguously solely from phonon dispersion curves. We show in this section that the EELS cross section indicates that the S-Ni spacing is 1.35 Å, in agreement with results of other spectroscopies.[20,23–26]

As mentioned earlier, the EELS cross section is dominated by the interference between loss amplitudes associated with the S layer and the Ni layer below. That this is the case is supported by the fact the cross section is a rapid function of incident electron energy, momentum transfer $\mathbf{q}_{\parallel}$, and the scattering angles $(\theta_i,\phi_i,\theta_f,\phi_f)$. The

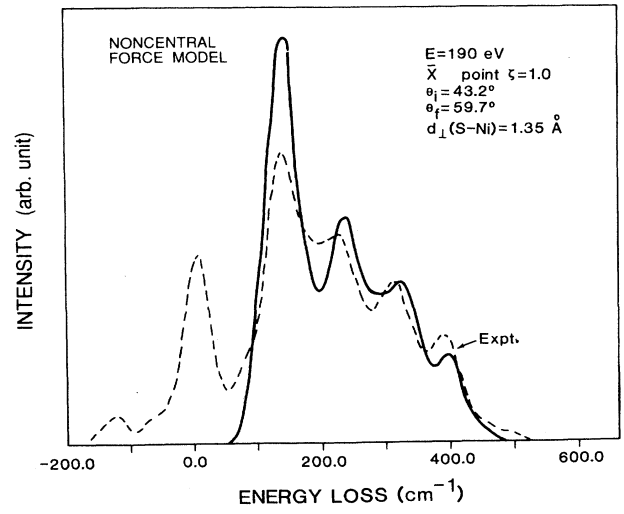

FIG. 10. Similar to Fig. 9 for $E=190$ eV.

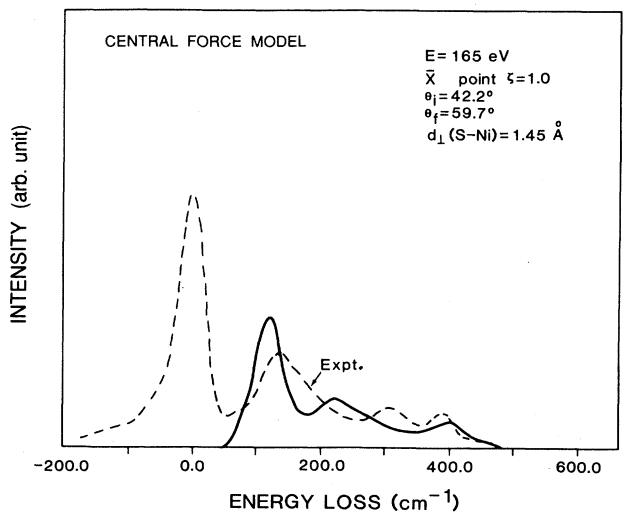

FIG. 11. Calculated (solid line) and measured (dashed line) EELS cross-section spectra for $E=165$ eV and $\zeta=1.0$ ($\bar{X}$ point). The atomic displacement amplitudes based on a central-force lattice dynamical model and $d_{\text{S-Ni}}=1.45$ Å are used for the EELS cross-section calculations.

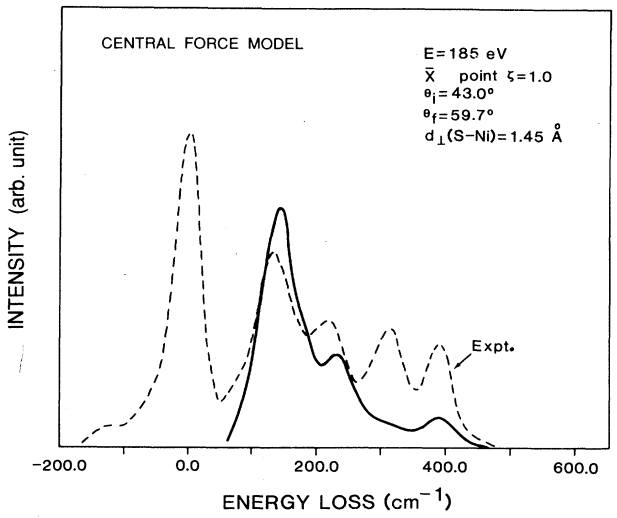

FIG. 13. Similar to Fig. 11 for $E=185$ eV.

loss amplitude of an individual layer is a much slower function. The calculated cross sections at $\bar{X}$ using displacement amplitudes of the central-force model with $d_{\text{S-Ni}}=1.35$ Å are shown in Figs. 4–8. The scattering plane is $\bar{\Gamma}\bar{X}$. The calculation and experiment are done for $E=150$–190 eV, in increments of 5 eV. To save space, Figs. 4–8 show only five selected energies. The calculated cross section of individual surface and antinode AIB modes are indicated as vertical lines while the solid curve is the Gaussian-broadened sum of all the lines. Following the dependence of the cross section of individual modes, we see that at low energies (155–170 eV), the relative intensities of the AIB modes R_1, R_2 are quite large. Note that the S_5 mode, which has a nonzero inelastic-electron-scattering cross section due to the four-fold hollow site of the S atom appears in between the R_1 and R_2 modes.[27] At higher energies (185–190 eV), the relative intensities of the S_{6L} and $S_{\parallel}$ even surface modes become strong. Such behaviors are closely matched in the data (dashed lines). The experimental peak at 0.0 cm^{-1} is due to residual geometric disorder which for adsorbate superstructures is typically somewhat larger than for clean surfaces is not included in the theoretical model.

If we keep the S-Ni spacing at 1.35 Å, and use displacement amplitudes of the non-central-force model, we obtain practically similar calculated EELS cross-section

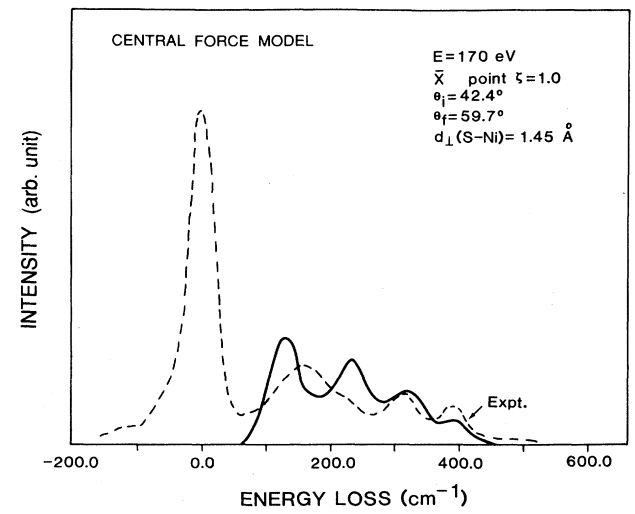

FIG. 12. Similar to Fig. 11 for $E=170$ eV.

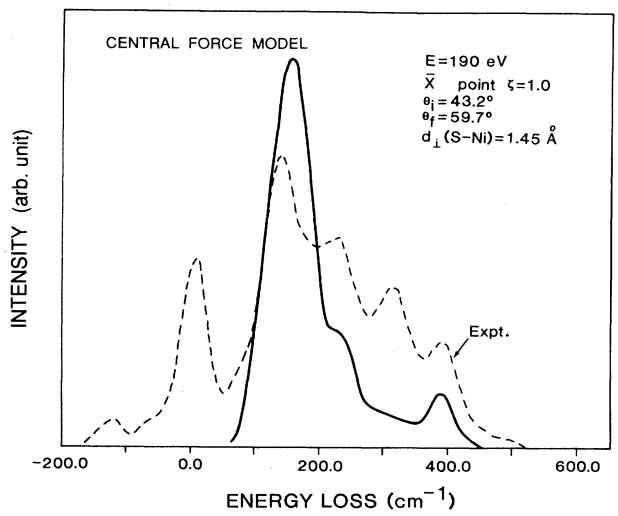

FIG. 14. Similar to Fig. 11 for $E=190$ eV.

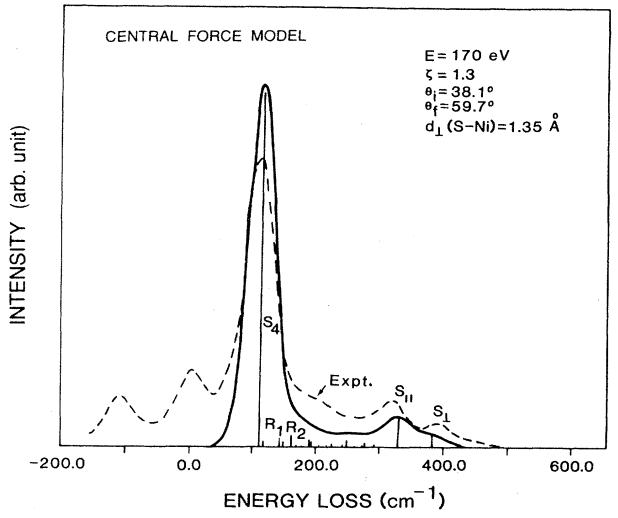

FIG. 15. Calculated (solid line) and measured (dashed line) EELS cross-section spectra for $E=170$ eV and $\zeta=1.3$. (Central-force lattice dynamical model, $d_{\text{S-Ni}}=1.35$ Å.)

spectra. The spectra at $\bar{X}$ for selected energies are shown in Figs. 9 and 10. However, if we change the Ni-S spacing to 1.45 Å and use the corresponding central-force model displacement amplitudes, we obtain calculated EELS spectra in gross disagreement with the data. The comparison of the EELS spectra for selected energies are shown in Figs. 11–14. At low energies (165-170 eV), the calculated cross sections of the antinode AIB modes are too small, while that of the S_{6L} mode is too strong. At high energies, the calculated cross section of the $S_{\parallel}$ even mode is much too weak. These comparison clearly indi-

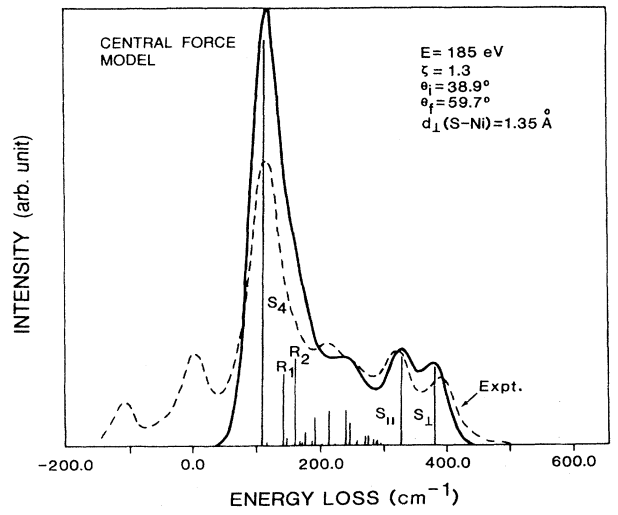

FIG. 16. Similar to Fig. 15 for $E=185$ eV.

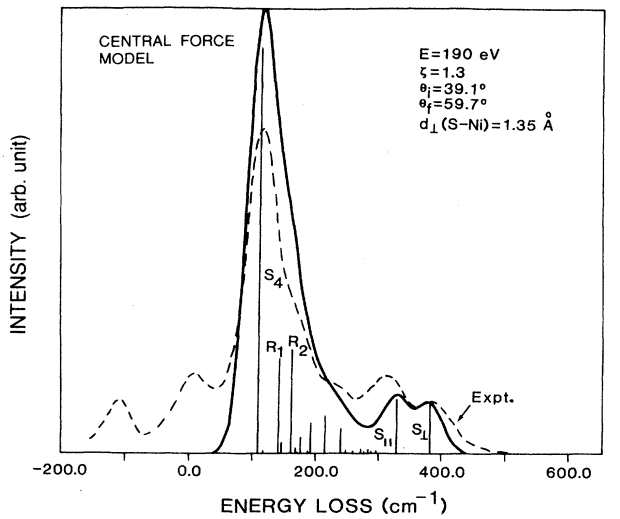

FIG. 17. Similar to Fig. 15 for $E=190$ eV.

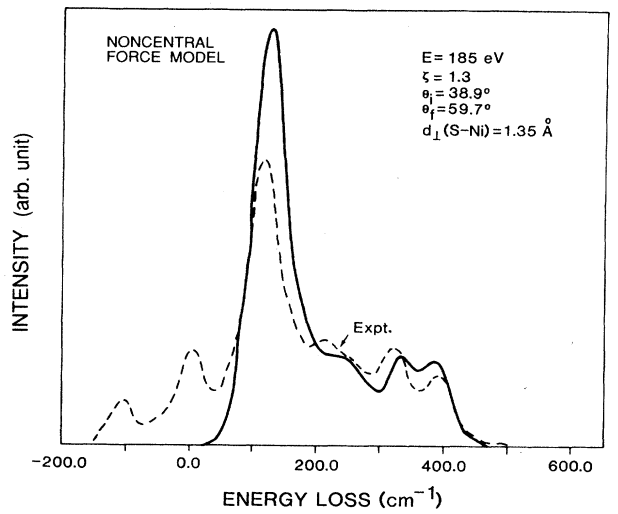

FIG. 18. Calculated (solid line) and measured (dashed line) EELS cross-section spectra for $E=185$ eV and $\zeta=1.3$. (Non-central-force lattice dynamical model, $d_{\text{S-Ni}}=1.35$ Å.)

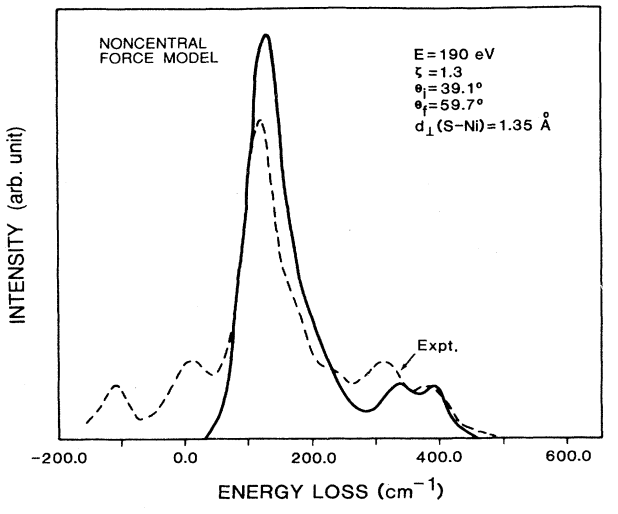

FIG. 19. Similar to Fig. 18 for $E=190$ eV.

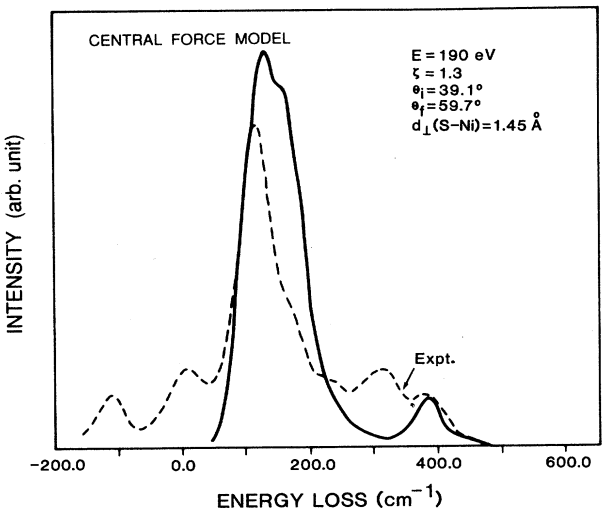

FIG. 20. Calculated (solid line) and measured (dashed line) EELS cross-section spectra for $E=185$ eV and $\zeta=1.3$. (Central-force lattice dynamical model, $d_{S\text{-}Ni}=1.45$ Å).

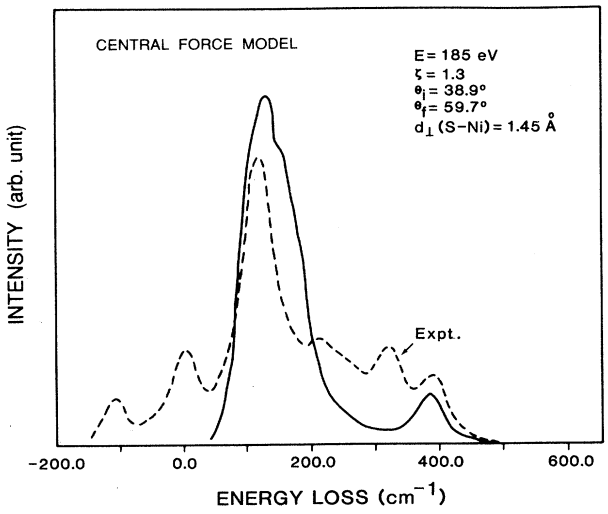

FIG. 21. Similar to Fig. 20 for $E=190$ eV.

cate that agreement between theory and experiment is obtained for the EELS spectra if S is placed at a height of 1.35 Å above the Ni layer. This structural result, based on comparing calculated EELS cross sections with experiment, is independent of the lattice dynamical models.

We have carried out similar analysis at $\zeta=\mathbf{q}_{\parallel}/1.26$ Å$^{-1}=1.3$. The experiments were actually performed by moving from $\bar{X}$ towards the (01) beam. We note that the eigenfrequencies $\omega(\zeta=0.7)=\omega(\zeta=1.3)$, while the displacement amplitudes at $\zeta=1.3$ are complex conjugates of those at $\zeta=0.7$. The comparisons between theory and experiment for S-Ni spacing at 1.35 Å are shown in Figs. 15–17 for central force model eigendisplacements and in Figs. 18 and 19 for non-central-force-model eigendisplacements, respectively. Again, there is good correspondence between theory and experiment. The antinode AIB mode R_2 is now stronger than R_1. If we put S at 1.45 Å above the Ni layer, the calculated EELS spectra show strong disagreement with the data. Two examples are shown in Figs. 20 and 21. In particular, we see that the calculated cross sections for the S_{6L} and $S_{\parallel}$ modes are too weak.

VI. SUMMARY

We have shown that the electron-energy-loss cross sections are sensitive indicators of the S-Ni spacing. By comparing measured EELS spectra with calculated cross sections, the adsorption height of $c(2\times2)$S on Ni(001) is determined at 1.35 Å. This structural determination is unambiguous in spite of the fact that the correct lattice dynamical model for the system is unknown.

The extensive EELS spectra used in this study were measured at $\bar{X}$ and $\zeta=1.3$. The non-central-force model used here is, at best, an *ad hoc* explanation. We need more complete data at $\bar{\Gamma}$ to properly determine the correct lattice dynamical model for this system. Such work is under current investigation.

ACKNOWLEDGMENTS

We thank Dr. J. E. Black for proposing the non-central-force model as a possible explanation for fitting the measured dispersion curves. This work is supported by the U.S. Department of Energy Grant No. DE-FG02-84ER45147 and the Petroleum Research Fund Grant No. 1154-AC5,6. Y.C. acknowledges partial support by IBM.

*Present address: Lawrence Berkeley Laboratory, University of California, Berkeley, CA 94720.

†Permanent address: Dipartimento di Fisica, Università degli Studi di Genova, via Dodecaneso 33, I-16146 Genova, Italy.

[1]J. P. Toennies, J. Vac. Sci. Technol. A **2**, 1055 (1984).

[2]S. Lehwald, J. M. Szeftel, H. Ibach, T. S. Rahman, and D. L. Mills, Phys. Rev. Lett. **50**, 518 (1983).

[3]H. Ibach and D. L. Mills, *Electron Spectroscopy and Surface Vibrations* (Academic, New York, 1982).

[4]S. Y. Tong, C. H. Li, and D. L. Mills, Phys. Rev. Lett. **44**, 407 (1980).

[5]C. H. Li, S. Y. Tong, and D. L. Mills, Phys. Rev. B **21**, 3057 (1980).

[6]S. Y. Tong, C. H. Li, and D. L. Mills, Phys. Rev. B **24**, 806 (1981).

[7]M. L. Xu, B. M. Hall, S. Y. Tong, M. Rocca, H. Ibach, S. Lehwald, and J. E. Black, Phys. Rev. Lett. **54**, 1171 (1985).

[8]B. M. Hall and D. L. Mills, Phys. Rev. B **34**, 8318 (1986).

[9]S. Lehwald, F. Wolf, H. Ibach, B. M. Hall, and D. L. Mills, Surf. Sci. **192**, 131 (1987).

[10]L. L. Kesmodel, M. L. Xu, and S. Y. Tong, Phys. Rev. B **34**, 2010 (1986).

[11]M. H. Mohamed, L. L. Kesmodel, B. M. Hall, and D. L. Mills, Phys. Rev. B **37**, 2763 (1988).

[12]Y. Chen, Z. Q. Wu, M. L. Xu, S. Y. Tong, K.-M. Ho, and X.-W. Wang, Phys. Rev. B **37**, 9978 (1988).

[13]An exception is the pair of S_5 modes, whose cross sections come entirely from the motion of second-layer Ni atoms.
[14]S. Y. Tong, in *Progress in Surface Science*, edited by S. G. Davisson (Pergamon, Oxford, 1975).
[15]S. Lehwald, M. Rocca, H. Ibach, and T. S. Rahman, Phys. Rev. B **31**, 3477 (1985).
[16]H. Ibach, J. Vac. Sci. Technol. A **5**, 419 (1987).
[17]S. Y. Tong and L. L. Kesmodel, Phys. Rev. B **8**, 3753 (1973).
[18]S. Y. Tong, J. B. Pendry, and L. L. Kesmodel, Surf. Sci. **54**, 21 (1976).
[19]M. A. Van Hove and S. Y. Tong, J. Vac. Sci. Technol. **12**, 231 (1975).
[20]D. H. Rosenblatt, J. G. Tobin, H. G. Mason, R. F. Davis, D. A. Shirley, C. H. Li, and S. Y. Tong, Phys. Rev. B **23**, 3828 (1981).
[21]J. E. Black (private communication).
[22]M. L. Xu and S. Y. Tong, J. Vac. Sci. Technol. A **4**, 1302 (1986).
[23]J. E. Demuth, D. W. Jepsen, and P. M. Marcus, Phys. Rev. Lett. **31**, 540 (1973).
[24]S. Brennan, J. Stöhr, and R. Jaeger, Phys. Rev. B **24**, 4871 (1981).
[25]J. J. Barton, C. C. Bahr, Z. Hussain, S. W. Robey, J. G. Tobin, L. E. Klebanoff, and D. A. Shirley, Phys. Rev. Lett. **51**, 272 (1983).
[26]P. J. Orders, B. Sinković, C. S. Fadley, R. Trehan, Z. Hussain, and J. Lecante, Phys. Rev. B **30**, 1838 (1984).
[27]S. Y. Tong, Y. Chen, and Z. Q. Wu, Phys. Rev. B **38**, 2192 (1988).